Journal of Medicinal Chemistry

Letter

Rational Design of Non-Nucleoside, Potent, and Orally Bioavailable Adenosine Deaminase Inhibitors: Predicting Enzyme Conformational Change and Metabolism

Tadashi Terasaka, Kiyoshi Tsuji, Takeshi Kato, Isao Nakanishi, Takayoshi Kinoshita, Yasuko Kato, Masako Kuno, Takeshi Inoue, Kohichiro Tanaka, and Katsuya Nakamura

J. Med. Chem., **2005**, 48 (15), 4750-4753• DOI: 10.1021/jm050413g • Publication Date (Web): 24 June 2005

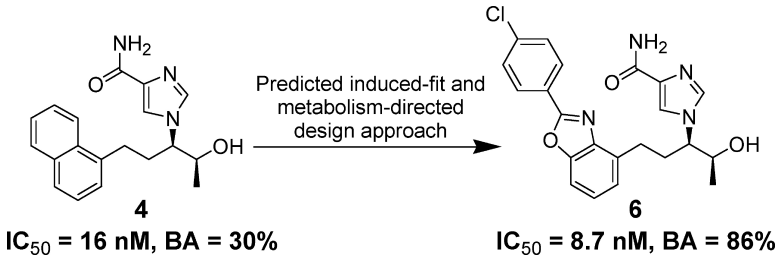

4
IC_{50} = 16 nM, BA = 30%

6
IC_{50} = 8.7 nM, BA = 86%

More About This Article

Additional resources and features associated with this article are available within the HTML version:

- Supporting Information
- Links to the 1 articles that cite this article, as of the time of this article download
- Access to high resolution figures
- Links to articles and content related to this article
- Copyright permission to reproduce figures and/or text from this article

View the Full Text HTML

Journal of Medicinal Chemistry is published by the American Chemical Society. 1155 Sixteenth Street N.W., Washington, DC 20036

Rational Design of Non-Nucleoside, Potent, and Orally Bioavailable Adenosine Deaminase Inhibitors: Predicting Enzyme Conformational Change and Metabolism

Tadashi Terasaka,*,† Kiyoshi Tsuji,† Takeshi Kato,† Isao Nakanishi,‡,# Takayoshi Kinoshita,‡ Yasuko Kato,§ Masako Kuno,§ Takeshi Inoue,§ Kohichiro Tanaka,|| and Katsuya Nakamura†

Medicinal Chemistry Research Laboratories, Basic Research Laboratories, Medicinal Biology Research Laboratories, and Biopharmaceutical and Pharmacokinetic Research Laboratories, Fujisawa Pharmaceutical Co., Ltd., 2-1-6, Kashima, Yodogawa-ku, Osaka 532-8514, Japan

Received May 2, 2005

Abstract: From metabolic considerations and prediction of an inhibitor-induced conformational change, novel adenosine deaminase (ADA) inhibitors with improved activities and oral bioavailability have been developed on the basis of our originally designed non-nucleoside ADA inhibitors. They demonstrated in vivo efficacy in models of inflammation and lymphoma. Furthermore, X-ray crystal structure analysis has revealed a novel induced fit to ADA.

Adenosine is an endogenous purine nucleoside released by cells and has a wide variety of biological activities such as immunosuppressive properties, protective effects in cerebral and myocardial ischemia, and inhibitory effects in lymphoproliferation. In recent years, adenosine has also been considered as an important factor in the attenuation of inflammation,[1,2] which is signaled through the A2a adenosine receptor. Adenosine deaminase (ADA) (EC 3.5.4.4) is a ubiquitous purine metabolic enzyme that catalyzes the irreversible deamination of adenosine and 2′-deoxyadenosine to inosine and 2′-deoxyinosine, respectively.[3] ADA exists as cytosolic and extracellular forms and has an important role in regulating intra- and extracellular adenosine concentrations. It is well-known that ADA deficiency results in severe combined immunodeficiency by accumulation of lymphotoxic adenosine and 2′-deoxyadenosine.[4] From a pharmacology viewpoint, ADA inhibition has interest as potential therapy of malignant leukemia and lymphomas. Furthermore, it is considered that ADA inhibiton has great potential for anti-inflammatory drugs with few side effects by preventing adenosine released specifically at inflamed sites from metabolism by extracellular ADA, colocalized on the cell surface with CD26, which is strongly up-regulated following T-cell activation and is known as the T-cell activation marker. [5]

Although a number of ADA inhibitors are known (e.g., pentostatin,[6] (+)-EHNA,[7] and various derivatives[8]), they have many problems such as poor pharmacokinetics[9] and several toxicities.[10] Pentostatin, which is the only ADA inhibitor in clinical use, is only available via intravenous administration,[11] and moreover, use is limited to the treatment of adult patients with hairy cell leukemia. Therefore, we initiated a search for ADA inhibitors with reduced toxicity and oral bioavailability by changing the nucleoside framework of the known inhibitors to a non-nucleoside framework. A recent report from our laboratories described the discovery of a good lead compound **1** (IC_{50} = 570 nM, human ADA) for optimization because of its simple, non-nucleoside framework.[12] Rational lead hybridization of **1** with the structurally distinct random screening hit **2** (IC_{50} = 700 nM)[12] and further efforts using a structure-based approach resulted in the discovery of the novel non-nucleoside ADA inhibitor **3** (Figure 1).[13] Although it had a high potency in terms of ADA inhibitory activity, the oral bioavailability was too poor for clinical use (IC_{50} = 6.7 nM, bioavailability BA = 10%). On the other hand, we also discovered potent and orally bioavailable ADA inhibitors **4** (IC_{50} = 16 nM, BA = 30%) and **5** (IC_{50} = 15 nM, BA = 44%) by a structure-based and metabolism-directed design approach based on **1**.[14] Furthermore, **5** demonstrated in vivo efficacy in models of inflammation and lymphoma after oral administration (po) for the first time. However, it was still not sufficient in terms of inhibitory activity and pharmacokinetics because **5** at 32 mg/kg po twice daily dosing (b.i.d.) was needed to show the same in vivo antitumor activity in a SCID mouse model[15] as intraperitoneal administration (ip) of pentostatin at 2.5 mg/kg once daily dosing (u.i.d.). Therefore, we attempted further design of more improved ADA inhibitors based on structure−activity relationships (SAR) and structural information of inhibitor/ADA complexes obtained in our original studies. In this communication, we report the discovery of improved potent and orally bioavailable ADA inhibitors by a predicted induced fit and metabolism-directed design approach and disclose a novel binding mode for ADA by a conformational change at the active site.

Compound **5** was designed on the basis of the crystal structure complexed with ADA and metabolic study of **4** to retain high inhibitory activity and to improve pharmacokinetics. That is, according to the crystal structure of the **4**/ADA complex, the enzyme had undergone conformational change, the same as in the **2**/ADA complex, and formed binding pockets (F1 and F2) that were spatially distinct from the pockets utilized by substrate-like inhibitors (Figure 3a−c).[16] In consideration of the narrow planar hydrophobic space available at F1 and protection from metabolism, a 2,3-dichlorophenyl ring was introduced in place of the naphthyl ring of **4**.[14] The resulting **5** showed potent inhibitory activity similar to that of **4** (Figure 2, Table 1). Although the naphthyl and 2,3-dichlorophenyl rings were bound to the F1 space, these moieties are located at the entrance position of the enzyme and do not utilize the F1 space sufficiently. Moreover, the hydrophobic

* To whom correspondence should be addressed. Phone: +81-6-6390-1286. Fax: +81-6-6304-5414. E-mail: tadashi.terasaka@jp.astellas.com.
† Medicinal Chemistry Research Laboratories.
‡ Basic Research Laboratories.
# Current address: Department of Theoretical Drug Design, Graduate School of Pharmaceutical Sciences, Kyoto University, Sakyo-ku, Kyoto 606-8501, Japan.
§ Medicinal Biology Research Laboratories.
|| Biopharmaceutical and Pharmacokinetic Research Laboratories.

10.1021/jm050413g CCC: $30.25
Published on Web 06/24/2005

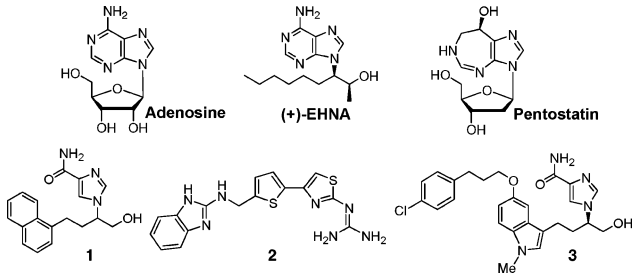

Figure 1. Chemical structures of adenosine and known ADA inhibitors.

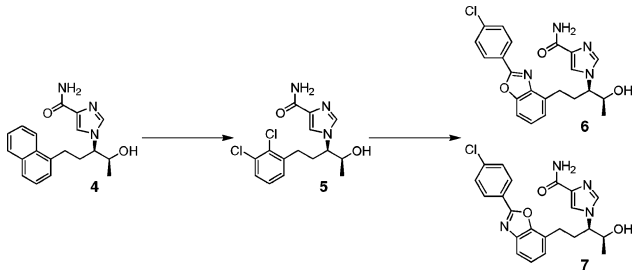

Figure 2. Design process for discovery of **6** and **7**.

space of F2, which is occupied by the benzimidazole ring of **2**, was also not utilized in the binding of **4** and **5** (parts b and c of Figure 3). It was considered that utilizing these hydrophobic spaces contributed to the enhancement of the inhibitory activities by gaining further van der Waals or hydrophobic interactions. However, we have also experienced from a previous study that utilizing the F2 space contributes to enhancement of the inhibitory activities and also resulted in increased molecular weight and disadvantages for pharmacokinetic improvement.[12,13] For metabolic stability, it is necessary to remove the easily metabolized parts from the designed compounds.[14] It was considered that utilizing F1 hydrophobic space in binding with ADA is effective. Therefore, on the basis of our original information, we next planned to make the best use of the narrow planar hydrophobic F1 space and block metabolism of the designed compounds to enhance activity and improve pharmacokinetics. As a result, **6** and **7** were designed, as shown in Figure 2. That is, in consideration of the narrow planar hydrophobic space available at F1 and protection of the designed compound from metabolism (oxidation of the naphthyl ring was predicted from the metabolic study of **4**), the naphthyl ring of **4** was replaced with a benzoxazolyl ring. Furthermore, the 2-position of the benzoxazolyl ring was substituted with a *p*-chlorophenyl ring directly because introduction of a halogen atom at the para position of the phenyl ring can protect from metabolism.[17] According to replacement of the naphthyl ring of **4** with 2-(4-chlorophenyl)-benzoxazolyl rings of the designed compounds based on the **4**/ADA complex, they could not be accommodated to the binding site because they have a rigid and planar structure at the 2-(4-chlorophenyl)benzoxazolyl moiety and thus the *p*-chlorophenyl ring clashes with the inner wall of F1 pocket (Figure 3d). However, we predicted from previously obtained information of crystal structure analyses of ADA complexes with our inhibitors that the enzyme can change the shape of the F1 pocket. In the substrate-like inhibitor/ADA complex, the active site is perfectly enclosed by the lid consisting of the loop (Ala183-Ile188) and two leucine side chains (Leu58 and 62) from an α-helix (Thr57-Ala73). It was considered that the lid was closed to accommodate the substrates. On the other hand, ADA performed an induced fit to bind our inhibitors by opening the lid and formed the hydrophobic binding pockets (F1 and F2).[12−14] Therefore, the shape of the F1 pocket is somewhat changeable depending on the inhibitor structure. In our previously disclosed crystal structures of inhibitor/ADA complexes, although the wall formed by Leu62 and the loop in the substrate-like inhibitor/ADA complex was opened, the inner wall of the F1 pocket is still formed by Leu 58 and Asp 185. However, Asp 185 is flexible because it is placed in the loop region of the enzyme. Moreover, it was considered that the interaction between Leu 58 and Asp 185 was weak (Figure 4).

Therefore, we considered that these residues can be pushed out in order to bind a rigid structure such as **6** and **7**. As a result, they may be able to not only accommodate in the enzyme active site but also use further hydrophobic space for binding. Thus, **6** and **7** were actually synthesized and evaluated. Consequently, they showed 2-fold more potent inhibitory activities than **4** and **5** (Table 1). A crystal structure of the **7**/ADA complex verified our prediction about inhibitor-induced change of the binding site (Figure 3e,f). That is, the benzoxazolyl ring was bound to the F1 space, the same as the naphthyl ring of **4**, and the inner wall of the F1 pocket expanded outside the active site to accommodate the *p*-chlorophenyl ring of **7**. Moreover, interestingly, the F2 space was diminished compared to that of our previously designed inhibitor/ADA complexes. Despite the conformational changes, the other parts showed the same binding mode as **4**. This binding mode was previously unknown and is spatially distinct from that of substrate-like inhibitors (Figure 3a) and our previously reported inhibitors (Figure 3b,c).

Because the primary objective of this study was discovery of ADA inhibitors with superior pharmacokinetics compared to **5**, compounds **6** and **7** with higher potency than **4** and **5** were subjected to pharmacokinetic experiments (Table 1). They displayed improved and/or the same metabolic stability to in vitro clearance in liver microsomes compared to **4** and **5**. Moreover, **6** and **7** had drastically improved pharmacokinetics and exceeded **5** in most pharmacokinetic parameters, as shown in Table 1. Upon dosing of **6** (10 mg/kg) to rats, drastic improvements in maximum plasma concentration (C_{max} = 14.72 μg/mL) and area under the blood concentration−time curve (AUC = 56.23 μg·h/mL) were observed. Despite the same metabolic stability to in vitro clearance as **5**, dosing of **7** (10 mg/kg) to rats showed a substantial improvement of C_{max} (5.58 μg/mL) and plasma half-life ($t_{1/2}$ = 3.45 h) and led to a drastic improvement of AUC (29.56 μg·h/mL) (BA = 52%). In particular, **6** displays excellent oral bioavailability in rats and dogs (BA = 86% and 81%, respectively).

The in vivo antitumor activity of our best compound **6** was next evaluated in a SCID mouse lymphoma model[15] (Table 2). Oral administration of **6** with the antitumor 9-β-D-arabinofuranosyladenine (AraA) at 10 and 32 mg/kg u.i.d. resulted in prolonged survival with a median survival time (MST) of 43.0 and 45.5 days, respectively. The mice not only survived significantly longer than control mice (MST of 22.0 days) but was

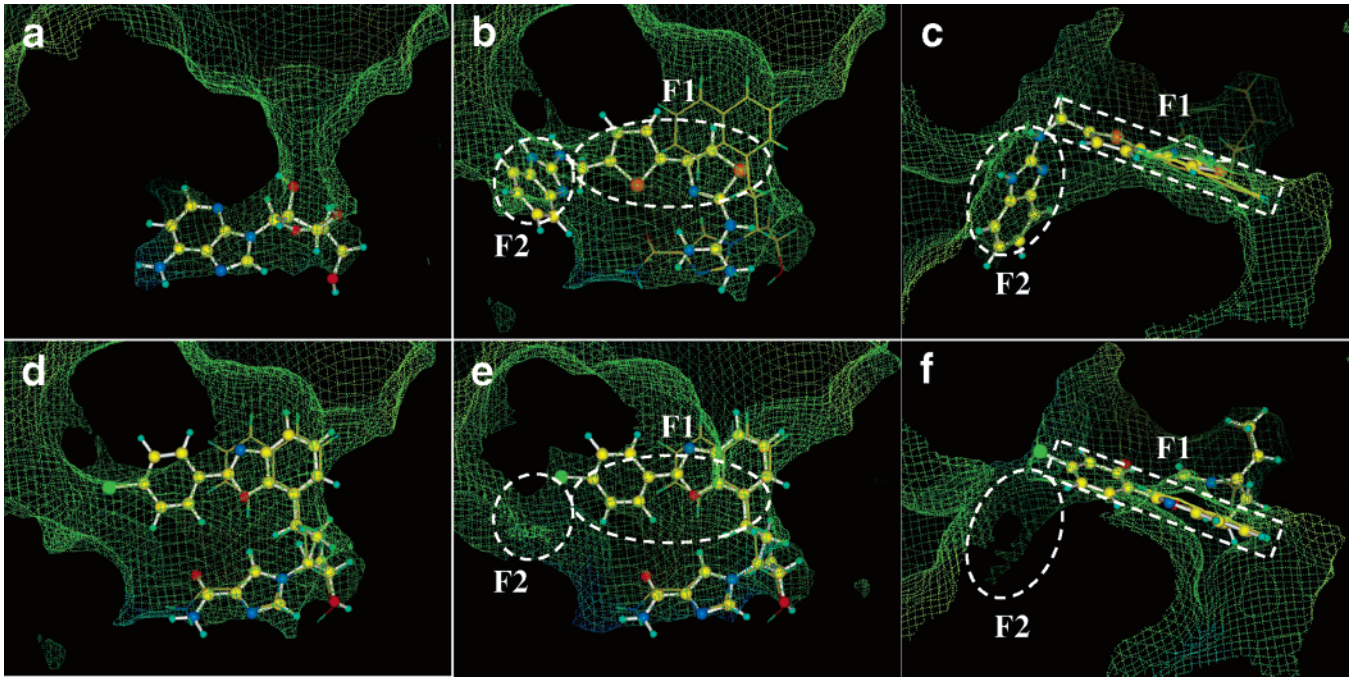

Figure 3. Binding mode of inhibitors at the ADA active site. Accessible surfaces of the carbon atoms at the active sites are drawn by mesh. The upper portions of (a), (b), (d), and (e) are the active site entrance (solvent region), and the other nonmeshed black regions are occupied by protein. (a) Binding mode of 1-deazaadenosine to the active site of the substrate analogue/ADA complex. (b) Binding orientations of **2** and **4** superimposed onto the active site surface of the **4**/ADA complex. (c) View from the active site entrance of (b). (d) Binding orientations of **7** and **4** superimposed onto the active site surface of the **4**/ADA complex. (e) Binding orientation of **7** and **4** superimposed onto the active site surface of the **7**/ADA complex. (f) View from the active site entrance of (e).

Table 1. In Vitro Clearance with Liver Microsomes of Rat, Dog, and Human, and Pharmacokinetic Parameters of **3**−**7** after po Administration to Rats and Dogs (10 mg/kg, $n = 2-3$)

		in vitro clearance (mL min^{-1} kg^{-1})[b]			pharmacokinetics parameters in rats[b]			BA (%)[c]	
compd	IC_{50} (nM)[a]	rat	dog	human	C_{max} (μg/mL)	$t_{1/2}$ (h)	AUC_{0-24h} (μg·h/mL)	rat	dog
3	6.7	643	nd[d]	nd[d]	0.21	1.09	0.26	10	nd[d]
4	16	307	30	45	1.25	0.66	1.37	30	38
5	15	111	21	4.5	1.63	1.66	2.11	44	43
6[e]	8.7	50	6.2	12	14.72	1.87	56.23	86	81
7	8.6	131	6.0	34	5.58	3.45	29.56	52	50

[a] IC_{50} values were measured with human ADA. Assays were performed in duplicate. [b] See Supporting Information. [c] BA = bioavailability. [d] nd = not determined. [e] HCl salt.

better than **5** because **6** at 10 mg/kg po u.i.d. exhibited antitumor activity against lymphoma in combination with AraA comparable to that observed for **5** at 32 mg/kg po b.i.d. and intraperitoneal administration of pentostatin at 2.5 mg/kg.

Furthermore, **6** and **7** were evaluated in an in vivo model of inflammation. In the adjuvant arthritis model in rats, both showed anti-inflammatory effects orally (ED_{30} = 0.3 and 0.6 mg/kg po, respectively), and these efficacies were improved compared to that of **5** (ED_{30} = 1.6 mg/kg po).

The syntheses of **6** and **7** are outlined in Scheme 1. The Wittig−Horner reaction between phosphonate **8**[18] and the suitable arylaldehyde gave pentenone **9**. Stereoselective reduction of the ketone moiety was accomplished with L-selectride in THF, followed by catalytic hydrogenation with palladium on carbon (Pd−C) in EtOAc to afford the corresponding secondary alcohols **11**. **12** was prepared by procedures similar to that of **4** in our recent report.[14] **6** and **7** were obtained by removal of the *tert*-butyldimethylsilyl (TBS) group of the corresponding **12** with tetrabutylammonium fluoride (TBAF).

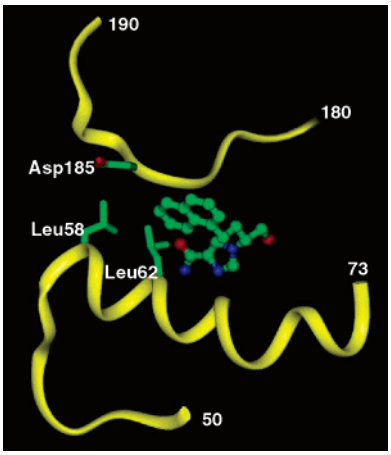

Figure 4. "Lid" of the active site of the **1**/ADA complex (PDB code, 1NDY). The backbone atoms of residues 50−73 and residues 180−190 are represented by ribbons, and several residues consisting of the lid are drawn in stick form. Compound **1** is in ball-and-stick form. Residue numbers of both ends of the backbones are also indicated.

In summary, we report further efforts starting from the novel non-nucleoside ADA inhibitor **4** and discovered

Table 2. Comparative Antitumor Activity of Compounds **5** and **6** and Pentostatin in U-937 Lymphoma Model

drug	dose (mg/kg)[b]	MST (day)
control		22.0
AraA	10	23.5
5[a] (po)	10 (b.i.d.)	34.0
	32 (b.i.d.)	42.5
	32 (u.i.d.)	38.0
6[a] (po)	10 (u.i.d.)	43.0
	32 (u.i.d.)	45.5
pentostatin (ip)	0.25	34.0
	2.5	42.5

[a] HCl salt. [b] b.i.d. = twice daily dosing. u.i.d. = once daily dosing.

Scheme 1[a]

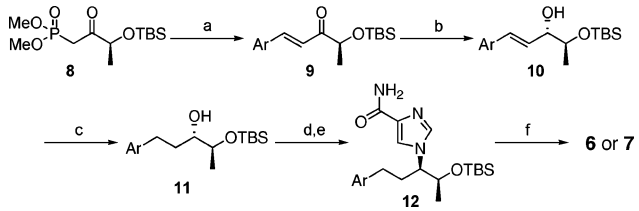

[a] Reagents and conditions: (a) ArCHO, *n*-BuLi, THF, 0 °C to room temp, overnight; (b) L-selectride, THF, −20 °C, 30 min; (c) H_2/Pd−C, EtOAc, room temp, 1 h; (d) MsCl, Et_3N, CH_2Cl_2, 0 °C, 1 h; (e) 4-imidazolecarboxamide, NaH, DMF, 80 °C, 24 h to 3 days; (f) TBAF, THF, 0 °C, 1 h.

two inhibitors with potent activities and drastically improved oral bioavailability from metabolic considerations and prediction of an inhibitor-induced conformational change. Consequently, they also demonstrated improved in vivo efficacy in models of inflammation and lymphoma after oral administration. In particular, in the lymphoma model in mice, oral administration of **6** at 10 mg/kg once daily showed the same antitumor activity as intraperitoneal administration of pentostatin at 2.5 mg/kg. Moreover, the X-ray structure of the **7**/ADA complex revealed a novel conformation, which should be useful for the further design of novel ADA inhibitors.

Acknowledgment. The authors are grateful to The Chemo-Sero-Therapeutic Research Institute for the gift of pentostatin. We thank Dr. David Barrett for valuable comments and help in the preparation of the manuscript.

Supporting Information Available: Experimental details and analytical data of compounds. This material is available free of charge via the Internet at http://pubs.acs.org.

References

(1) Cronstein. B. N. Adenosine, an endogenous antiinflammatory agent. *J. Appl. Physiol.* **1994**, *76*, 5−13.
(2) Ohta, A.; Sitkovsky, M. Role of G-protein-coupled adenosine receptors in downregulation of inflammation and protection from tissue damage. *Nature* **2001**, *414*, 916−920.
(3) Cristalli, G.; Costanzi, S.; Lambertucci, C.; Lupidi, G.; Vittori, S.; Volpini, R.; Camaioni, E. Adenosine deaminase: Functional implications and different classes of inhibitors. *Med. Res. Rev.* **2001**, *21*, 105−128.
(4) Resta, R.; Thompson, L. F. SCID: the role of adenosine deaminase deficiency. *Immunol. Today* **1997**, *18*, 371−374.
(5) Kameoka, J.; Tanaka, T.; Nojima, Y.; Schlossman, S. F.; Morimoto, C. Direct association of adenosine deaminase with T cell activation antigen, CD26. *Science* **1993**, *261*, 466−469.
(6) Agerwal, R. P.; Spector, T.; Parks, R. E. Tight-binding inhibitors. IV. Inhibition of adenosine deaminase by various inhibitors. *Biochem. Pharmacol.* **1977**, *26*, 359−367.
(7) (a) Baker, D. C.; Hanvey, J. C.; Hawkins, L. D.; Murphy, J. Identification of the bioactive enantiomer of *erythro*-3-(adenine-9-yl)-2-nonanol (EHNA), a semi-tight binding inhibitor of adenosine deaminase. *Biochem. Pharmacol.* **1981**, *30*, 1159−1160. (b) Bessodes, M.; Bastian, G.; Abushanab, E.; Panzica, R. P.; Berman, S. F.; Marcaccio, E. J.; Chen, S. F.; Stoeckler, J. D.; Parks, R. J. Effect of chirality in erythro-9-(2-hydroxy-3-nonyl) adenine (EHNA) on adenosine deaminase inhibition. *Biochem. Pharmacol.* **1982**, *31*, 879−882.
(8) (a) Cristalli, G.; Eleuteri, A.; Franchetti, P.; Grifantini, M.; Vittori, S.; Lupidi, G. Adenosine deaminase inhibitors: Synthesis and structure−activity relationships of imidazole analogue of erythro-9-(2-hydroxy-3-nonyl)adenine. *J. Med. Chem.* **1991**, *34*, 1187−1192. (b) Pragnacharyulu, P. V. P.; Varkhedkar, V.; Curtis, M. A.; Chang, I. F.; Abushanab, E. Adenosine deaminase inhibitors: Synthesis and biological evaluation of unsaturated, aromatic, and oxo derivatives of (+)-erythro-9-(2′*S*-hydroxy-3′*R*-nonyl) adenine [(+)-EHNA]. *J. Med. Chem.* **2000**, *43*, 4694−4700.
(9) (a) McConnell, W. R.; Furner, R. L.; Hill, D. L. Pharmacokinetics of 2′-deoxycoformycin in normal and L1210 leukemic mice. *Drug Metab. Dispos.* **1979**, *7*, 11−13. (b) Lathia, C.; Fleming, G. F.; Meyer, M.; Ratain, M. J.; Whitfield, L. Pentostatin pharmacokinetics and dosing recommendations in patients with mild renal impairment. *Cancer Chemother. Pharmacol.* **2002**, *50*, 121−126. (c) McConnell, W. R.; El-Dareer, S. M.; Hill, D. L. Metabolism and disposition of *erythro*-9-(2-hydroxy-3-nonyl)[^{14}C] adenine in the rhesus monkey. *Drug Metab. Dispos.* **1980**, *8*, 5−7. (d) Lambe, C. U.; Nelson, D. J. Pharmacokinetics of inhibition of adenosine deaminase by *erythro*-9-(2-hydroxy-3-nonyl) adenine in CBA mice. *Biochem. Pharmacol.* **1982**, *31*, 535−539.
(10) Brogden, R. N.; Sorkin, E. M. Pentostatin. A review of its pharmacodynamic and pharmacokinetic properties, and therapeutic potential in lymphoproliferative disorders. *Drugs* **1993**, *46*, 652−677.
(11) Rafel, M.; Cervantes, F.; Beltran, J. M.; Zuazu, J.; Nieto, L. H.; Rayon, C.; Talavera, J. G.; Montserrat, E. Deoxycoformycin in the treatment of patients with hairy cell leukemia. *Cancer* **2000**, *88*, 352−357.
(12) Terasaka, T.; Kinoshita, T.; Kuno, M.; Nakanishi, I. A highly potent non-nucleoside adenosine deaminase inhibitor: Efficient drug discovery by intentional lead hybridization. *J. Am. Chem. Soc.* **2004**, *126*, 34−35.
(13) Terasaka, T.; Kinoshita, T.; Kuno, M.; Seki, N.; Tanaka, K.; Nakanishi, I. Structure-based design, synthesis, and structure−activity relationship studies of novel non-nucleoside adenosine deaminase inhibitors. *J. Med. Chem.* **2004**, *47*, 3730−3743.
(14) Terasaka, T.; Okumura, H.; Tsuji, K.; Kato, T.; Nakanishi, I.; Kinoshita, T.; Kato, Y.; Kuno, M.; Seki, N.; Naoe, Y.; Inoue, T.; Tanaka, K.; Nakamura, K. Structure-based design and synthesis of non-nucleoside, potent, and orally bioavailable adenosine deaminase inhibitors. *J. Med. Chem.* **2004**, *47*, 2728−2731.
(15) Niitsu, N.; Yamamoto-Yamaguchi, Y.; Kasukabe, T.; Okabe-Kado, J. Umeda, M.; Honma, Y. Antileukemic efficacy of 2′-deoxycoformycin in monocytic leukemia cells. *Blood* **2000**, *96*, 1512−1516.
(16) (a) Kinoshita, T.; Nishio, N.; Sato, A.; Murata, M. Crystallization and preliminary analysis of bovine adenosine deaminase. *Acta Crystallogr.* **1999**, *D55*, 2031−2032. (b) Kinoshita, T.; Nishio, N.; Nakanishi, I.; Sato, A.; Fujii, T. Crystal structure of bovine adenosine deaminase complexed with 6-hydroxyl-1,6-dihydropurine riboside. *Acta Crystallogr.* **2003**, *D59*, 299−303.
(17) Smith, D. A.; Jones, B. C.; Walker, D. K. Design of drugs involving the concepts and theories of drug metabolism and pharmacokinetics. *Med. Res. Rev.* **1996**, *16*, 243−266.
(18) Shapiro, G.; Buechler, D.; Hennet, S. Synthesis of enantiomerically pure muscarine analogs. *Tetrahedron Lett.* **1990**, *31*, 5733−5736.

JM050413G